ESO Science Archive Facility - Phase 3 Data Release Description
ESO public survey programme VANDELS - A deep VIMOS survey of the CANDELS UDS and CDFS fields, Data Release DR4
provided by R. McLure, submitted on 2021-01-29, published on 2021-02-04

Data Collection	<VANDELS>
Release Number	<4>
Data Provider	<Ross McLure, Laura Pentericci>
Date	<19.01.2021>

Abstract

This is the fourth and final data release (DR4) of the VANDELS survey, an ESO public spectroscopy survey targeting the high-redshift Universe. The VANDELS survey used the VIMOS spectrograph on ESO's VLT to obtain ultra-deep, medium resolution, optical spectra of galaxies within the UKIDSS Ultra Deep Survey (UDS) and Chandra Deep Field South (CDFS) survey fields (0.2 sq. degree total area). Using robust photometric redshift pre-selection, VANDELS targeted ≈2100 galaxies in the redshift interval 1.0<z<7.0, with 85% of its targets selected to be at z≥3. In addition, VANDELS targeted a substantial number of passive galaxies in the redshift interval 1.0<z<2.5. Exploiting the red sensitivity of the refurbished VIMOS spectrograph, the survey obtained ultra-deep optical spectroscopy with the VIMOS MR grism and GG475 order-sorting filter, which covers the wavelength range 4800-10000Å at a dispersion of 2.5 Å/pix and a spectral resolution of R~600. Each galaxy received between a minimum of 20-hours and a maximum of 80-hours of on-source integration time. The fundamental aim of the survey was to provide the high signal-to-noise spectra necessary to measure key physical properties such as stellar population ages, metallicities and outflow velocities from detailed absorption-line studies. By targeting two extra-galactic survey fields with superb multi-wavelength imaging data, VANDELS was designed to produce a unique legacy dataset for exploring the physics underpinning high-redshift galaxy evolution**.** A full description of the survey definition and first data release can be found in McLure et al. (2018) and Pentericci et al. (2018), respectively. A full description of the final data release can be found in:

"The VANDELS ESO public spectroscopic survey: final data release of 2087 spectra and spectroscopic measurements"
Garilli et al., 2021, A&A, in press, arXiv:2101.07645

Overview of Observations

The VANDELS survey targeted a total of eight VIMOS pointings, four pointings in the UDS field and four pointings in the CDFS field (see Fig. 1). Each VANDELS pointing had four associated masks, each of which was observed for 20-hours of on-source integration time. The survey utilized a nested slit allocation policy, such that the brightest objects within a given pointing appeared on a single mask (receiving 20-hours of integration), fainter objects appeared on two masks (receiving 40-hours of integration) and the faintest objects appeared on all four masks (receiving 80-hours of integration).

All observations were obtained using OBs designed to deliver a total of one-hour of on-source integration time. Each OB consisted of three integrations of 1200s, obtained in a three-point dither pattern, with dither off-sets of 0.82 arcseconds (dither positions 0,-0.82,1.64) corresponding to 4 pixels. One arc and one flat were obtained for calibration after the execution of two consecutive OBs. A spectrophotometric standard was observed at least once every 7 nights and at least once per run.

The nominal observing conditions required for a single exposure to be validated were: moon illumination below 0.5, seeing below 1.0 arcsecond FWHM, airmass below 1.5 and clear weather conditions. An exposure was still validated if one (and only one) of the above conditions was not met by less than 20% (e.g. seeing<1.2") and all other conditions were satisfied (see Fig. 2)

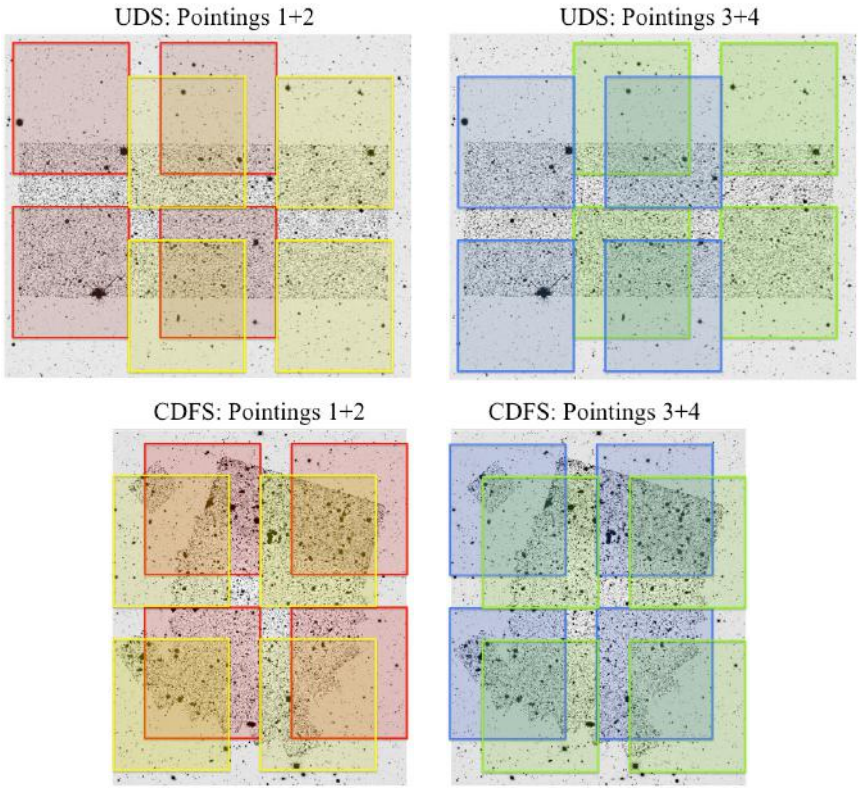


Fig 1. Layout of the eight VIMOS pointings within the UDS (top) and CDFS (bottom) fields. In each panel the background greyscale images show both the available *HST* (centre) and ground-based *H*-band imaging.

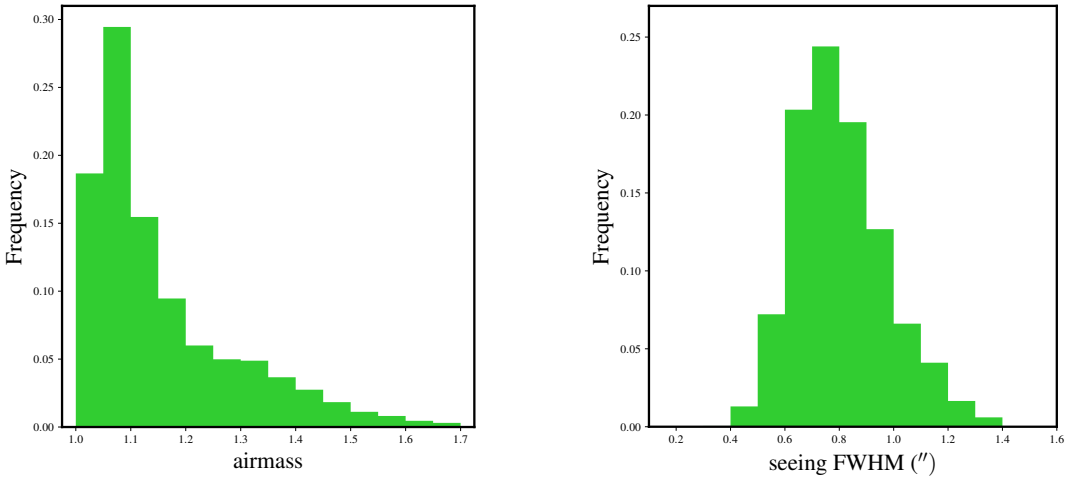


Fig 2. The left-hand and right-hand panels show histograms of the airmass and seeing for the observations obtained during the VANDELS survey, respectively.

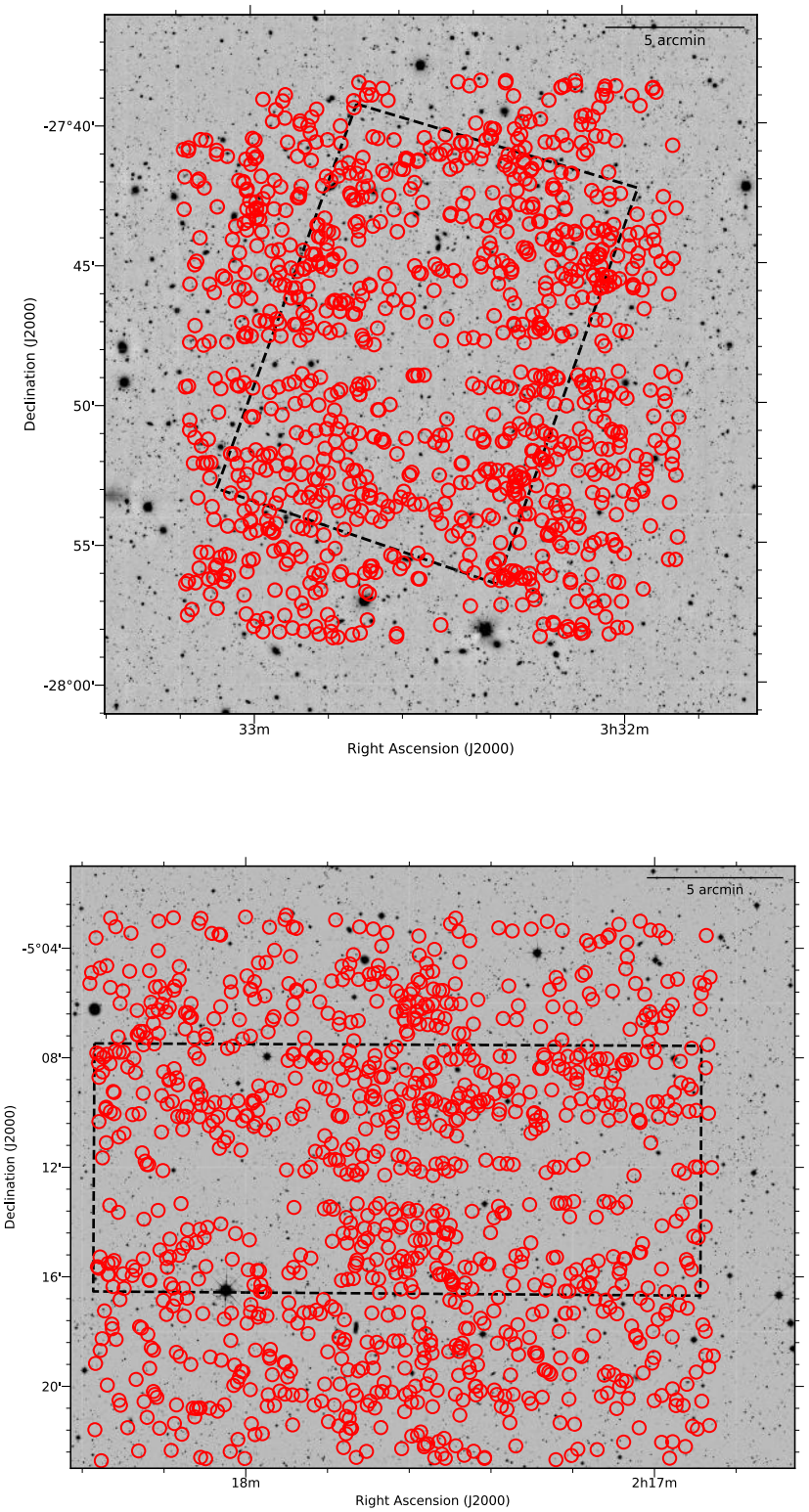


Fig. 3 Finding charts showing the location of the VANDELS DR4 spectra (red circles) within the CDFS (top) and UDS (bottom) fields. There are 1061 spectra in the CDFS and 1104 spectra in the UDS. The black dashed rectangles show the approximate location of the CANDELS near-IR Hubble Space Telescope imaging (Grogin et al. 2011). The background images are ground-based *H*-band data from the VISTA VIDEO survey (Jarvis et al. 2013) and UKIDSS UDS survey (Almaini et al., in prep) in the top and bottom panels respectively.

Object Classification

All of the VANDELS targets were selected based on their photometric redshift and their i, *z & H*-band magnitudes (full details can be found in McLure et al. 2018). There are six target classifications in total (listed below), but the vast majority of the VANDELS spectra fall into the first three classes.

CLASS = PASS_1.0_z_2.5 UVJ selected passive galaxies with $1.0 < z_{phot} < 2.5$, $H_{AB}<22.5$, $i_{AB}<25$

CLASS = SF_2.4<z<5.5 Bright star-forming galaxies with $2.4< z_{phot}<5.5$, $i_{AB}<25$

CLASS = LBG_3.0<z<5.5 Fainter star-forming galaxies with $3.0< z_{phot}< 5.5$, $H_{AB}<27$, $i_{AB}<27.5$

CLASS = LBG_5.5<z<7.0 Fainter star-forming galaxies with $5.5< z_{phot}< 7.0$, $H_{AB}<27$, $z_{AB}<27.5$

CLASS = AGN X-ray or IRAC-selected AGN candidates with $z_{phot}>2.4$, $i_{AB}<27.5$

CLASS = HERSCHEL Herschel detected galaxies with $z_{phot}>2.4$, $i_{AB}<27.5$

Release Content

This data release consists of spectra obtained during the three VANDELS observing seasons, ESO run numbers: 194.A-2003(E-T), which ran from Aug 2015-Jan 2016, Aug 2016-Feb 2017 and Aug 2017-Dec 2017.

This fourth data release consists of 2165 spectra. With respect to the previous release, DR4 provides spectra of 287 new targets and 104 spectra of serendipitously observed objects. In total the VANDELS Phase3 collection now includes 2165 spectra (1061 in CDFS and 1104 in UDS).

The data release consists of

- *Fully wavelength and flux calibrated 1D spectra for all 2165 galaxies, along with the associated error spectrum and sky spectrum.*
- *Wavelength calibrated 2D spectra for all 2165 galaxies.*
- *Catalogues listing the data associated with each galaxy (details below).*

Release Notes

Data Reduction and Calibration

VANDELS data reduction and calibration was performed with a fully-automated pipeline, starting from the raw data and flowing down to the wavelength- and flux-calibrated spectra. The pipeline, called *Easylife,* is an updated version of the algorithms and dataflow from the original VIPGI system, fully described in Scodeggio et al. (2005). A full description of the data reduction and calibration can be found in Garilli et al. (2021).

Spectroscopic Redshifts

Spectroscopic redshifts and associated quality flags have been determined for all objects in the current release using the Pandora software package, within the EZ environment (Garilli et al. 2010). The software simultaneously displays the 1D extracted spectrum, the 2D linearly resampled spectrum, the 1D sky spectrum and the noise. It is also possible to inspect the image thumbnail of the object with the exact position of the slit, to check for the presence of other sources in the same slit. The core algorithm for redshift determination is template cross-correlation, compared with a sepa-

rate estimate of an emission line redshift when applicable. A key element for the cross-correlation engine to deliver a robust measurement is the availability of reference templates that cover a wide range of galaxy and star types and a wide range of rest-frame wavelengths. To determine the VANDELS spectroscopic redshifts we adopted templates derived from previous VIMOS observations for the VVDS (Le Fèvre et al. 2013) and *z*COSMOS surveys (Lilly et al. 2007), with and without Lyman-α emission. Where necessary, it was also possible to set the redshift manually, e.g. by locating a single emission line in the spectrum.
In several cases, it was necessary to manually perform some cleaning of the spectra, i.e. removing obvious noise residuals at the location of strong sky lines, or the zero-order projection.

Each target was assigned to two measurers from the VANDELS team who independently determined the redshift and located the main spectral features (in emission or absorption). Each measurer also assigned a spectroscopic quality flag to the target: these quality flags have been allocated according to the original system devised for the VVDS and are related to the confidence of the spectral measurement. The reliability flag may take the following values:

- 0: No redshift could be assigned (set to Nan)
- 1: 50% probability to be correct
- 2: 75% probability to be correct
- 3: 95% probability to be correct
- 4: 100% probability to be correct
- 9: spectrum with a single emission line. The redshift given is the most probable given the observed continuum, it has a >80% probability to be correct.

The quality flags for AGN spectra are preceded by an additional 1 (e.g 12, 14 etc), the quality flags for spectra which were not primary targets are preceded by an additional 2 and the quality flags for spectra deemed to be problematic are preceded by an additional -1. A detailed analysis of the robustness of the spectroscopic quality flags based on the DR4 release can be found in Garilli et al. (2021).

Following their independent redshift determinations, the two measurers were required to compare their redshifts and flags and to reconcile any differences. As a final step, all spectra were also independently re-checked by the two PIs and any discrepancies in the redshifts and quality flags were again reconciled. This final pass was especially necessary to homogenize the quality flags as much as possible. Based on repeated measurements, the typical accuracy of the spectroscopic redshift measurements is estimated to be +/- 0.0007 (Garilli et al. 2021).

Known issues

During testing of the flux calibration of the VANDELS spectra, it became clear that the blue end of the spectra (i.e. λ<5600Å) suffer from a systematic drop in flux when compared to the available photometry. The underlying cause for this loss of blue flux is still under investigation. For the purposes of this data release (as for DR1, DR2 and DR3) we have implemented an empirically derived correction which corrects for the flux loss on average.

The empirical correction, which has been applied to all of the DR4 spectra, is designed to ensure that the final spectra of bright star-forming galaxies in the redshift interval 2.4<z<3.0 display the expected power-law continuum slopes in the rest-frame wavelength range (1300Å < λ < 2400Å), which are independently confirmed from the available photometry. It should be noted that, compared to the three previous data releases, the empirical blue flux correction applied to the DR4 spectra has been revised and updated, based on the availability of a larger number of spectra of bright star-forming galaxies. Full details of the improved blue flux correction can be found in Garilli et al. (2021).

At the time of the data release, we believe that the spectra including the correction for blue flux loss represent our best calibration of the VANDELS spectra. However, for completeness, we are also making available the spectra without the blue flux correction as an additional column of the 1D spectra fits table.

Previous Releases

All files released in DR1 were totally replaced by files released in DR2. DR2 provided new versions of all files in DR1 and added 483 spectra of additional targets. The third data release (DR3) added 412 spectra of new targets and replaced 121 files present in DR2 because of increased exposure time.

This fourth data release (DR4) totally replaces all the files released in DR3 because of the new blue flux correction that has been applied to all spectra. Compared to DR3, a total of 287 new target spectra have been added, bringing the total number of target spectra to 2061 (1006 in CDFS and 1055 in UDS), 1937 of which have received 100% or more of their scheduled exposure time. An additional 104 serendipitously observed spectra have also been added (55 in CDFS and 49 in UDS). In total the VANDELS collection now features 2165 spectra (1061 in CDFS and 1104 in UDS).

References

Garilli et al., 2012, PASP, 124, 1232
Garilli et al., 2010, PASP, 122, 827
Garilli et al., 2021, A&A, in press, arXiv:2101.07645
Grogin et al., 2011, ApJS, 197, 35
Horne, 1986, PASP, 98, 609
Jarvis et al., 2013, MNRAS, 428, 1281
Le Fèvre et al., 2013, A&A, 559, 14
Le Fèvre et al., 2015, A&A, 576, 79
Lilly et al., 2007, ApJS, 172, 70
McLure et al., 2018, MNRAS, 479, 25
Pentericci et al., 2018, A&A, 616, 174
Scodeggio et al., 2005, PASP, 117, 1284

Data Format

Files Types

For each target the following data files are being released:

- the one-dimensional spectrum in FITS format, containing the following arrays
  - WAVE: wavelength in Angstroms (in air)
  - FLUX: 1D spectrum flux in erg cm^{-2} s^{-1} $angstrom^{-1}$
  - ERR: noise estimate in erg cm^{-2} s^{-1} $angstrom^{-1}$
  - UNCORR_FLUX: 1D spectrum flux uncorrected for blue flux loss (see Known issues)
  - SKY: the subtracted sky in counts

- the two-dimensional resampled and sky subtracted (but not flux calibrated and atmospheric extinction corrected) spectrum in FITS format.

Catalogue Columns

In addition to the one and two-dimensional spectra, we are releasing an associated catalogue divided into two tiles (*VANDELS_UDS_SPECTRO.fits and VANDELS_CDFS_SPECTRO.fits*). The catalogue columns are described in the following table. The first 14 columns provide basic information associated with the released spectra. The remaining columns provide multi-band photometry and physical parameters derived via SED fitting. While the photometry is made available for all spectra, the physical parameters are only available for primary targets with a measured spectroscopic redshift (i.e. zflg=1,2,3,4,9,14). A full description of the photometry and physical parameters can be found in Garilli et al. (2021).

NAME	DESCRIPTION	DATA TYPE	UNIT
id	Object ID	CHAR	
delta	J2000 Declination	DOUBLE	deg
alpha	J2000 Right Ascension	DOUBLE	deg
i_AB	i_AB selection magnitude	FLOAT	mag
i_FILTER	i_AB selection magnitude filter	CHAR	
z_AB	z_AB selection magnitude	FLOAT	mag
z_FILTER	z_AB selection magnitude filter	CHAR	
H_AB	H_AB selection magnitude	FLOAT	mag
H_FILTER	H_AB selection magnitude filter	CHAR	
t_schedtime	Total requested exposure time	INT	sec
t_exptime	Current total exposure time	FLOAT	sec
zphot	Photometric redshift	FLOAT	
zspec	Spectroscopic redshift	FLOAT	
zflg	Spectroscopic redshift quality flag	FLOAT	
U_VIMOS	U_VIMOS flux	DOUBLE	mJy
U_VIMOS_err	U_VIMOS flux error	DOUBLE	mJy
U_CFHT	U_CFHT flux	DOUBLE	mJy
U_CFHT_err	U_CFHT flux error	DOUBLE	mJy
F435W	F435W flux	DOUBLE	mJy
F435W_err	F435W flux error	DOUBLE	mJy
B_SUBARU	B_SUBARU flux	DOUBLE	mJy
B_SUBARU_err	B_SUBARU flux error	DOUBLE	mJy
B_WFI	B_WFI flux	DOUBLE	mJy
B_WFI_err	B_WFI flux error	DOUBLE	mJy
IA484	IA484 flux	DOUBLE	mJy
IA484_err	IA484 flux error	DOUBLE	mJy
IA527	IA527 flux	DOUBLE	mJy
IA527_err	IA527 flux error	DOUBLE	mJy
V_SUBARU	V_SUBARU flux	DOUBLE	mJy
V_SUBARU_err	V_SUBARU flux error	DOUBLE	mJy
IA598	IA598 flux	DOUBLE	mJy
IA598_err	IA598 flux error	DOUBLE	mJy
F606W	F606W flux	DOUBLE	mJy
F606W_err	F606W flux error	DOUBLE	mJy
IA624	IA624 flux	DOUBLE	mJy
IA624_err	IA624 flux error	DOUBLE	mJy
IA651	IA651 flux	DOUBLE	mJy
IA651_err	IA651 flux error	DOUBLE	mJy
R_VIMOS	R_VIMOS flux	DOUBLE	mJy
R_VIMOS_err	R_VIMOS flux error	DOUBLE	mJy
R_SUBARU	R_SUBARU flux	DOUBLE	mJy
R_SUBARU_err	R_SUBARU flux error	DOUBLE	mJy
IA679	IA679 flux	DOUBLE	mJy
IA679_err	IA679 flux error	DOUBLE	mJy
IA738	IA738 flux	DOUBLE	mJy
IA738_err	IA738 flux error	DOUBLE	mJy
i_SUBARU	i_SUBARU flux	DOUBLE	mJy
i_SUBARU_err	i_SUBARU flux error	DOUBLE	mJy
F775W	F775W flux	DOUBLE	mJy

F775W_err	F775W flux error	DOUBLE	mJy
IA767	IA767 flux	DOUBLE	mJy
IA767_err	IA767 flux error	DOUBLE	mJy
F814W	F814W flux	DOUBLE	mJy
F814W_err	F814W flux error	DOUBLE	mJy
Z_VISTA	Z_VISTA flux	DOUBLE	mJy
Z_VISTA_err	Z_VISTA flux error	DOUBLE	mJy
F850LP	F850LP flux	DOUBLE	mJy
F850LP_err	F850LP flux error	DOUBLE	mJy
z_SUBARU	z_SUBARU flux	DOUBLE	mJy
z_SUBARU_err	z_SUBARU flux error	DOUBLE	mJy
znew_SUBARU	znew_SUBARU flux	DOUBLE	mJy
znew_SUBARU_err	znew_SUBARU flux error	DOUBLE	mJy
nb921	nb921 flux	DOUBLE	mJy
nb921_err	nb921 flux error	DOUBLE	mJy
F098M	F098M flux	DOUBLE	mJy
F098M_err	F098M flux error	DOUBLE	mJy
Y_HAWKI	Y_HAWKI flux	DOUBLE	mJy
Y_HAWKI_err	Y_HAWKI flux error	DOUBLE	mJy
Y_VISTA	Y_VISTA flux	DOUBLE	mJy
Y_VISTA_err	Y_VISTA flux error	DOUBLE	mJy
F105W	F105W flux	DOUBLE	mJy
F105W_err	F105W flux error	DOUBLE	mJy
F125W	F125W flux	DOUBLE	mJy
F125W_err	F125W flux error	DOUBLE	mJy
J_VISTA	J_VISTA flux	DOUBLE	mJy
J_VISTA_err	J_VISTA flux error	DOUBLE	mJy
J_WFCAM	J_WFCAM flux	DOUBLE	mJy
J_WFCAM_err	J_WFCAM flux error	DOUBLE	mJy
F160W	F160W flux	DOUBLE	mJy
F160W_err	F160W flux error	DOUBLE	mJy
H_VISTA	H_VISTA flux	DOUBLE	mJy
H_VISTA_err	H_VISTA flux error	DOUBLE	mJy
H_WFCAM	H_WFCAM flux	DOUBLE	mJy
H_WFCAM_err	H_WFCAM flux error	DOUBLE	mJy
Ks_HAWKI	Ks_HAWKI flux	DOUBLE	mJy
Ks_HAWKI_err	Ks_HAWKI flux error	DOUBLE	mJy
Ks_VISTA	Ks_VISTA flux	DOUBLE	mJy
Ks_VISTA_err	Ks_VISTA flux error	DOUBLE	mJy
Ks_ISAAC	Ks_ISAAC flux	DOUBLE	mJy
Ks_ISAAC_err	Ks_ISAAC flux error	DOUBLE	mJy
K_WFCAM	K_WFCAM flux	DOUBLE	mJy
K_WFCAM_err	K_WFCAM flux error	DOUBLE	mJy
CH1_IRAC	CH1_IRAC flux	DOUBLE	mJy
CH1_IRAC_err	CH1_IRAC flux error	DOUBLE	mJy
CH2_IRAC	CH2_IRAC flux	DOUBLE	mJy
CH2_IRAC_err	CH2_IRAC flux error	DOUBLE	mJy
dust_Av_16	V-band dust attenuation in magnitudes (16% percentile)	DOUBLE	mag
dust_Av_50	V-band dust attenuation in magnitudes (50% percentile)	DOUBLE	mag
dust_Av_84	V-band dust attenuation in magnitudes (84% percentile)	DOUBLE	mag
exponential_age_16	Time since the onset of star formation (16% percentile)	DOUBLE	Gyr
exponential_age_50	Time since the onset of star formation (50% percentile)	DOUBLE	Gyr
exponential_age_84	Time since the onset of star formation (84% percentile)	DOUBLE	Gyr
exponential_massformed_16	Total stellar mass formed (16% percentile)	DOUBLE	log(solMass)
exponential_massformed_50	Total stellar mass formed (50% percentile)	DOUBLE	log(solMass)
exponential_massformed_84	Total stellar mass formed (84% percentile)	DOUBLE	log(solMass)
exponential_tau_16	Exponential timescale for the SFH (16% percentile)	DOUBLE	Gyr
exponential_tau_50	Exponential timescale for the SFH (50% percentile)	DOUBLE	Gyr
exponential_tau_84	Exponential timescale for the SFH (84% percentile)	DOUBLE	Gyr
stellar_mass_16	Mass in living stars and remnants (16% percentile)	DOUBLE	log(solMass)
stellar_mass_50	Mass in living stars and remnants (50% percentile)	DOUBLE	log(solMass)
stellar_mass_84	Mass in living stars and remnants (84% percentile)	DOUBLE	log(solMass)
sfr_16	Star formation rate averaged over the last 100 Myr	DOUBLE	solMass/yr
sfr_50	Star formation rate averaged over the last 100 Myr	DOUBLE	solMass/yr

sfr_84	Star formation rate averaged over the last 100 Myr	DOUBLE	solMass/yr
ssfr_16	Specific SFR (16% percentile)	DOUBLE	log(yr**(-1))
ssfr_50	Specific SFR (50% percentile)	DOUBLE	log(yr**(-1))
ssfr_84	Specific SFR (84% percentile)	DOUBLE	log(yr**(-1))
UV_16	U-V colour adopting Williams et al. (2009) filters	DOUBLE	mag
UV_50	U-V colour adopting Williams et al. (2009) filters	DOUBLE	mag
UV_84	U-V colour adopting Williams et al. (2009) filters	DOUBLE	mag
VJ_16	V-J colour adopting Williams et al. (2009) filters	DOUBLE	mag
VJ_50	V-J colour adopting Williams et al. (2009) filters	DOUBLE	mag
VJ_84	V-J colour adopting Williams et al. (2009) filters	DOUBLE	mag
chisq_phot	Raw minimum chi-squared value for the fit to the d	DOUBLE	
n_bands	Number of photometric bands used in the fit	INT	
FILENAME	FITS filename of the spectrum	CHAR	

Due to the heterogeneous nature of the ground-based and space-based imaging covering the UDS and CDFS survey fields, the i_AB, z_AB and H_AB magnitudes listed in the release catalogues are generated from a number of different filters. The fundamental reason for this is the different photometry available for those targets selected within the areas covered by HST imaging (UDS_HST and CDFS_HST, ID numbers < 50,000) and those targets selected within the wider areas, primarily covered by ground-based imaging (UDS_GROUND and CDFS_GROUND, ID numbers > 100,000). Below we provide a guide to matching the catalogue photometry with the original filters:

- i_AB magnitudes refer to the SUBARU i'-filter for the UDS_GROUND and UDS_HST targets, the F775W filter for CDFS_HST targets and the SUBARU IA738 filter for the CDFS_GROUND targets.

- z_AB magnitudes refer to the SUBARU z'-filter for the UDS_GROUND and UDS_HST targets and the F850LP filter for the CDFS_GROUND and CDFS_HST targets.

- H_AB magnitudes refer to the F160W filter for the UDS_HST and CDFS_HST targets, the WFCAM H-filter for the UDS_GROUND targets and the VISTA H-filter for the CDFS_GROUND targets.

For each object, the origin of the i_AB, z_AB and H_AB photometry is listed in the catalogue in the i_FILTER, z_FILTER and H_FILTER columns.

Due to changing observing conditions, some masks in both the UDS and CDFS fields have received more than their nominally scheduled 20 hours of on-source integration, resulting in objects in the catalogue with t_exptime > t_schedtime. In addition, to optimize slit allocation, 144 objects in this data release where placed on multiple VIMOS masks and received 1.5-5.0 times their nominal integration time.

Acknowledgements

Any publication making use of this data, whether obtained from the ESO archive or via third parties, must include the following acknowledgement:

- "Based on data products created from observations collected at the European Organisation for Astronomical Research in the Southern Hemisphere under ESO programme 194.A-2003(E-T)"

If the access to the ESO Science Archive Facility services was helpful for you research, please include the following acknowledgement:

- "This research has made use of the services of the ESO Science Archive Facility."

Science data products from the ESO archive may be distributed by third parties, and disseminated via other services, according to the terms of the Creative Commons Attribution 4.0 International license. Credit to the ESO origin of the data must be acknowledged, and the file headers preserved.